

1 **Extending thermal response test assessments with inverse numerical modeling of**
2 **temperature profiles measured in ground heat exchangers**

3 J. Raymond^{a,1}, L. Lamarche^b and M. Malo^a

4 ^a*Institut national de la recherche scientifique, Centre Eau Terre Environnement, 490 rue*
5 *de la Couronne, Québec (Qc), G1K 9A9, Canada*

6 ^b*Département de génie mécanique, École de Technologie Supérieure, 1100 rue Notre-*
7 *Dame Ouest, Montréal (Qc), H3C 1K3, Canada*

8 **Abstract**

9 Thermal response tests conducted to assess the subsurface thermal conductivity for the
10 design of geothermal heat pumps are most commonly limited to a single test per
11 borefield, although the subsurface properties can spatially vary. The test radius of
12 influence is additionally restricted to 1~2 m, even though the thermal conductivity
13 assessment is used to design the complete borefield of a system covering at least tens of
14 squared meters. This work objective was therefore to develop a method to extend the
15 subsurface thermal conductivity assessment obtained from a thermal response test to
16 another ground heat exchanger located on the same site by analyzing temperature profiles
17 in equilibrium with the subsurface. The measured temperature profiles are reproduced
18 with inverse numerical simulations of conductive heat transfer to assess the site basal heat
19 flow, at the location of the thermal response test, and evaluate the subsurface thermal
20 conductivity, beyond the thermal response test. Paleoclimatic temperature changes and
21 topography at surface were considered in the model that was validated by comparing the
22 thermal conductivity estimate obtained from the optimization process to that of a
23 conventional thermal response test.

24 **Keywords:** geothermal, heat pump, heat exchanger, thermal response test, temperature
25 profile, thermal conductivity.

¹ Corresponding author: Tel.: +1 418 654 2559; fax: + 1 418 654 2600.
E-mail address: jasmin.raymond@inrs.ca (J. Raymond).

26 **1. Introduction**

27 Thermal response tests (TRTs), envisioned in the early 80's [1] and fully developed with
28 mobile apparatus in the 90's [2,3], are now commonly performed to evaluate the
29 subsurface thermal conductivity to design ground source heat pump systems. The test
30 consists of disturbing the subsurface temperature with the circulation of heated water in a
31 pilot ground heat exchanger (GHE) installed before the complete borefield of a given
32 building is fully constructed [4]. Water flow rate circulating in the GHE and temperature
33 at its inlet and outlet are analyzed to infer the bulk subsurface thermal conductivity [5,6].
34 This parameter is a key to determine the length of ground heat exchanger required to
35 fulfill the energy needs of a building. TRTs are consequently performed for prefeasibility
36 studies to design ground source heat pump systems and evaluate their economic
37 viabilities.

38 The conventional TRT experiment conducted in the field aims at reproducing heat
39 transfer that can occur during the operation of a ground source heat pump system. A heat
40 injection rate of 50 to 80 W m⁻¹ of borehole to create a temperature difference of 3 to
41 7 °C between the inlet and outlet of the GHE is recommend in North American industry's
42 guidelines [7]. A source of high power varying from 8 to 12 kW is needed to operate the
43 heating element and the pump of the mobile apparatus. The testing unit and its fuel fired
44 generator commonly used to supply power are cumbersome. Mobilizing the equipment
45 in the field and performing the test is a significant expense, which have found limited
46 applications due to its cost. TRTs are mostly carried out for large ground source heat
47 pump systems were the uncertainty in GHE length can offset the cost of a test. One test is
48 typically conducted for the whole borefield and this single thermal conductivity

49 assessment is considered for design although the test radius of influence is limited to less
50 than 1~2 m [8] and the subsurface properties can vary with position at a given field due to
51 heterogeneities.

52 Recent efforts to develop competitive field tests carried out with GHEs in the scope of
53 geothermal system design resulted in the use of heating cables to inject heat underground
54 [9–11]. The pump is avoided for thermal response tests with heating cables and heat is
55 injected in the standing water column of the GHE, which can facilitate installation of the
56 equipment in the field. The use of a heating cable assembly enclosing sections of heating
57 and non-heating wires was further proposed to perform TRTs with a low power source in
58 GHEs that are commonly more than a hundred meter in length [12,13]. Although TRTs
59 with heating cables provide advantages that can help reducing the test cost, the duration
60 of a test enclosing 40 to 60 hours of heat injection followed by an equivalent duration of
61 thermal recovery remain its main limitation. Gamma ray log have been alternatively used
62 to infer the subsurface thermal conductivity at different depths [14]. Such wireline
63 geophysical log can potentially provide an instantaneous assessment method for the
64 subsurface thermal conductivity but borehole logging have to be performed in an open
65 hole without GHE piping. This limitation is important as pipe can be rapidly installed
66 after drilling to avoid collapsing of the borehole wall. The interpretation of a temperature
67 profile recorded in GHE at equilibrium with the subsurface was additionally proposed to
68 evaluate the subsurface thermal conductivity [15]. A wireless probe was developed for
69 that purpose to measure temperature as the probe sink along the pipe of a GHE [16]. The
70 analysis of equilibrium temperature profiles to determine the subsurface properties was,
71 in fact, achieved in the 70's to determine the thermostratigraphy of sedimentary rocks

72 [17]. Although measurements are fairly simple to perform in the field, the interpretation
73 of a temperature profile can be limited by inaccurate information about the Earth heat
74 flow, which is essential to analyze the temperature data. The measured temperature
75 gradient can further be affected by topography or by paleoclimatic temperature variations
76 at surface [18,19]. Thermal conductivity assessments with temperature profiling using
77 thermostratigraphic principles are consequently spatially limited, but deserve a broader
78 attention to diversify tools available for subsurface characterization in the scope of
79 geothermal system design. Previous studies described the use of temperature profiling
80 before and after a TRT in the same GHE to improve test analysis with the identification
81 of groundwater flow or vertical variations in subsurface thermal conductivity [20,21].
82 Temperature profiles can offer further advantages to extend the evaluation of subsurface
83 properties beyond the location of a single TRT, a topic that has not been fully addressed.
84 Evaluation of the subsurface thermal conductivity at more than one location on the same
85 site can be useful when designing large ground source heat pump systems including tens
86 to hundreds of boreholes drilled in a heterogeneous geological medium. Temperature
87 profiles that can be measured at a low cost with a submersible probe in GHEs provide
88 easily accessible data to infer the subsurface thermal conductivity without repeating
89 TRTs on the same site.

90 The analysis of temperature profiles measured in GHEs undisturbed by heat injection of a
91 TRT and in the absence of accurate information about the Earth heat flow was
92 investigated in this study. The objective of the work presented was to develop and verify
93 a methodology to evaluate the subsurface thermal conductivity from the temperature
94 profile of GHEs recorded with a wired probe and taking into account limitations arising

95 from the unknown site heat flow. Temperature measurements undisturbed by heat
96 injection were achieved in two GHEs located at the same site and that are approximately
97 140 m deep, a relatively shallow medium where the temperature gradient is affected by
98 topography and the recent climate warming. An inverse numerical analysis method was
99 developed to infer the Earth heat flow at the study site from the temperature profile and a
100 conventional TRT assessment conducted in a first GHE. The numerical simulations took
101 into account the site topography and the historical changes in ground surface temperature
102 that occurred over the past centuries. The same inverse modeling approach was then used
103 to analyze the temperature profile of the second GHE to evaluate the subsurface thermal
104 conductivity beyond the location of the TRT, considering the heat flow value inferred in
105 the first GHE. If the Earth heat flow was known at every surface location where
106 temperature had remained constant, Fourier's Law of heat conduction would be sufficient
107 to infer the subsurface thermal conductivity with an equilibrium temperature profile.
108 Such conditions are seldom if not never meet and the proposed method was developed to
109 overcome those constrains. The field and numerical analysis method relying on wired
110 temperature profiling is fully described in this manuscript, providing an original
111 contribution showing how to extend TRT assessments when more than one test has to be
112 conducted at the same site or within a region of similar heat flow.

113 **2. Site settings**

114 The work was conducted at a site where conventional TRTs has been performed before to
115 validate with experimental results the methodology developed for numerical inversion of
116 the temperature profiles. The site is located in Saint-Lazare-de-Bellechasse, in the
117 Appalachian geological province of Canada (Figure 1), and hosts two GHEs that have a

118 depth of 139 m. The GHEs are located 9 m from each other and were previously installed
119 to evaluate the performance of thermally enhance pipes [6]. The boreholes were drilled
120 until 150 m depth in a sequence constituted of a sandy overburden having a thickness of
121 10 m followed by mudslates layers of the Armagh Formation [22]. The diameter of the
122 boreholes that were backfilled with silica sand was 0.15 m and a single U-pipe having a
123 nominal diameter equal to 32 mm was installed until 139 m depth since the lower part of
124 the boreholes collapsed. Conventional TRT conducted on each borehole during 168 h of
125 heat injection flowed by 44 to 66 h of thermal recovery indicated a bulk subsurface
126 thermal conductivity equal to 3.0 and 3.5 W m⁻¹ K⁻¹ at the location of borehole PG-08-01
127 and PG-08-02, respectively [6].

128 The groundwater level was measured in the boreholes before installation of the GHEs at
129 0.72 m depth below the ground surface that is at an elevation of 301 m above sea
130 level (asl) near the GHEs. The site is on the flank of a northwest-southeast trending hill
131 that has an average slope of 3.3 % going downhill toward the northwest. A survey of the
132 groundwater well record for the area revealed a hydraulic gradient on the order of 0.03,
133 following the site topography.

134 Equilibrium heat flow map are unavailable for the area. The best information about heat
135 flow is from a map drawn at the country scale of Canada that suggest a heat flow in the
136 range of 20 to 50 mW m⁻² [23]. The nearest equilibrium heat flow measurement was
137 made at a distance of approximately 70 km, which evidences the difficulties in assessing
138 the site heat flow from regional maps. The ground surface temperature in the area has
139 increased over the past two-hundred years [24]. Joint inversion of temperature profiles
140 from 28 boreholes that are 600 m deep and located in Eastern Canada revealed a ground

141 surface temperature that slightly decreased before 1800 and then increased until now
142 [25]. Although this temperature trend was determined for a very large region of Western
143 Ontario and Eastern Québec in the vicinity of the studied site, it was assumed to be
144 representative of the site surface temperature fluctuations as climate trends are similar for
145 the area. Such a temperature evolution was essential to constrain the analysis of the
146 temperature profiles in the GHEs that are typically shorter than the boreholes used for
147 paleoclimatic reconstructions having at least 300 m depth.

148 **3. Methodology**

149 The thermal conductivity assessment from the TRT conducted in a first GHE was used to
150 find the site heat flow with inverse numerical simulations of conductive heat transfer to
151 reproduce the temperature profile measured in the GHE. The heat flow evaluation from
152 the first GHE simulations was then used as an input parameter to find the thermal
153 conductivity at the location of the second GHE with a similar modeling approach to
154 reproduce its temperature profile. The thermal conductivity obtained for the second GHE
155 with inverse modeling was finally compared to that obtain from the TRT conducted in
156 this second GHE to verify the accuracy of the methodology. The field and numerical
157 simulation methods are described below, providing guidelines to reproduce the method at
158 other sites (Figure 3).

159 **3.1 Field measurements**

160 Temperature profiles undisturbed by heat injection and at equilibrium with the subsurface
161 were measured with a submersible pressure and temperature data logger hooked to a wire
162 and lowered inside a pipe of each GHE. The temperature measurements for this study

163 were recorded after TRTs have been conducted since the purpose of the work was to
 164 validate the method at a site with existing subsurface information obtained from previous
 165 field testing. In a case where the method is actually used to extend thermal conductivity
 166 assessment in the context of geothermal system design, it is suggested to measure
 167 temperature profiles before the TRT. The submersible data logger used was a RBRduet
 168 with a fast temperature response, where the thermistor accuracy, resolution and time
 169 constant are $\pm 2 \times 10^{-3}$ °C, 5×10^{-5} °C and 1×10^{-1} s, respectively. The pressure sensor can go
 170 to a depth of 500 m and its accuracy and resolution for depth measurements are
 171 2.5×10^{-1} m and 5×10^{-3} m, respectively. The logger was set to record temperature and
 172 pressure every second and was gradually lowered in the GHE at a constant pace. Upon
 173 lowering the logger in the GHE, the water level inside the U-pipe slightly rises as the
 174 volume of the data logger and the wireline displaced the GHE water. This small water
 175 movement can affect the geothermal gradient measured in the GHE. The depth
 176 measurements were consequently corrected by subtracting the volume introduced in the
 177 U-pipe expressed in equivalent length with:

$$178 \quad D^*(L) = D - \left(\frac{V_{\text{logger}} + V_{\text{wire}}(L)}{2\pi r_{\text{pipe,in}}^2} \right) \quad \text{eq. 1}$$

179 where D^* and D (m) are the corrected and measured depth and V (m^3) is for the volume
 180 of the data logger and wireline that is expressed in equivalent length by dividing by two
 181 times the area inside a pipe considering its internal radius r (m). Note that the logger
 182 volume is constant and the wire volume increases with its length L (m) unwound in the
 183 GHE, which can be determined with the measured depth knowing the water and surface
 184 pipe elevations before lowering the probe. This depth correction assumes that the water

185 level rise in the GHE is faster than the time for the temperature of the water that rise in
186 the U-pipe to reach equilibrium with the subsurface temperature. The temperature profile
187 taking into account the corrected depth is tough to provide a measurement of the
188 geothermal gradient which can be repeated in each GHE of a given site. Those
189 observations offer the information needed to find the site heat flow and the subsurface
190 thermal conductivity at different GHEs with inverse numerical modeling if the subsurface
191 thermal conductivity from at least one borehole is known.

192 **3.2 Numerical simulations**

193 The temperature profile measured in a GHE was reproduced with a numerical simulation
194 of transient heat transfer in the subsurface using the finite element program COMSOL
195 Multiphysics [26]. Heat transfer in the GHE was not simulated since the models aimed at
196 reproducing temperature measurements that are in equilibrium with the subsurface
197 temperature. The transient conductive heat transfer equation was solved numerically in
198 two dimensions:

$$199 \quad \frac{\partial}{\partial x} \left(\lambda \frac{\partial T}{\partial x} \right) + \frac{\partial}{\partial y} \left(\lambda \frac{\partial T}{\partial y} \right) = \rho c \frac{\partial T}{\partial t} \quad \text{eq. 2}$$

200 where λ ($\text{W m}^{-1} \text{K}^{-1}$) is the thermal conductivity assumed to be isotropic, ρ (kg m^{-3}) is the
201 density and c ($\text{J kg}^{-1} \text{K}^{-1}$) is the heat capacity. Simulations were conducted over a domain
202 representing a cross-section of the subsurface at the studied site oriented in the direction
203 of the topographical slope (Figure 4). The thermal properties of the subsurface were
204 assumed to be uniform, constant with time, and heat generation due to decay of
205 radioactive elements inside the subsurface was neglected. The upper boundary of the

206 simulation domain was drawn according to the site topography and the borehole was
207 located at the center of the horizontal direction. The horizontal and vertical widths of the
208 model were selected to be 1000 m in length to minimize the influence of the vertical and
209 the bottom boundaries. The model mesh formed with triangles refined near the surface
210 for a better resolution at the borehole contained 3046 elements.

211 The boundary conditions were adiabatic at the vertical side walls, a constant heat flow at
212 the bottom and a uniform temperature at surface varying with time to reproduce
213 paleoclimatic changes in ground surface temperature over the past six centuries
214 (Figure 4). The constant heat flow boundary at the bottom represents the Earth natural
215 heat flow directed toward the surface. The upper surface temperature varying with time
216 was determined according to paleoclimatic reconstructions of the past six centuries that
217 have affected the temperature profile measured at the depth of the borehole. The initial
218 temperature condition was calculated according to the basal heat flow and the subsurface
219 thermal conductivity to represent the equilibrium geothermal gradient at steady state
220 before the recent surface warming disturbed the thermal state of the subsurface. The
221 temperature measured at the base of the GHEs, which is less influenced by the ground
222 surface temperature variations than the temperature in the upper section of the GHEs, was
223 extrapolated upward and downward according to the equilibrium geothermal gradient to
224 set the initial temperature distribution. This initial temperature condition was therefore
225 recalculated for every simulation where the basal heat flow or the subsurface thermal
226 conductivity was changed in the optimization process to reproduce the temperature
227 profile of the GHEs.

228 The simulations were conducted for a period of 615 y, with constant time steps of 5 y to
229 reproduce the surface warming and the propagation of the thermal disturbance in the
230 subsurface until the present moment, when the temperature profiles were measured in the
231 GHEs. In other words, the end of the simulations corresponded to the time when the
232 temperature measurements were taken and the simulations were for the historic 615 y
233 preceding the measurements. The time to complete a single simulation of the subsurface
234 temperature evolution was on the order of 20 s on a desk top computer with an Intel i5
235 3.33 GHz processor and 8 Go of random access memory. This fast simulation time
236 obtained with a light cross-section model allowed to conduct multiple simulations to find
237 the unknown basal heat flow and subsurface thermal conductivity with optimization of
238 the temperature profiles.

239 The basal heat flow was considered as unknown for simulations of the temperature
240 profile in the first GHE, whereas the thermal conductivity is assumed to be known and
241 taken from the TRT results. Identification of the proper basal heat flow is essential since
242 the simulations aim at reproducing the temperature of the subsurface for a heat tracing
243 experiment lasting centuries where the source of perturbations are paleoclimates. The
244 sum of squared residuals between the observed and simulated temperature profiles was
245 minimized with the coordinate search method [27] to find the basal heat flow that best
246 reproduced the observed temperatures. In this case, the optimization solver searches for
247 the minimum sum of squared residuals by constructing an estimate of the gradient and
248 performs a line search along this direction before attempting a new evaluation along the
249 coordinate direction. The optimality tolerance of the solver was set to 1×10^{-3} to 1×10^{-4}

250 and the maximum number of objective evaluations was determined to be 40, although the
251 solver always converged before the 40 iterations.

252 Once the basal heat flow was determined with the optimization of the temperature profile
253 in the first GHE with a known subsurface thermal conductivity, it was used as an input
254 for simulations of the temperature profile in the second GHE to find the subsurface
255 thermal conductivity at this location. The optimization process was similar, with the
256 minimization of the sum of squared residuals between the observed and simulated
257 temperatures using the coordinate search method to find, in this case, the thermal
258 conductivity. This inverse numerical simulation process allowed extrapolating the
259 thermal conductivity assessment obtained with a TRT at the location of the first GHE to
260 the location of the second GHE without doing a TRT and simply relying on temperature
261 profiling.

262 The assumptions involved in the simulation process can be synthesized as the following:

- 263 • Heat is transferred by conduction in 2D space and there is no internal heat
264 generation,
- 265 • Land use affecting the temperature at surface and the basal heat flow is similar
266 among the boreholes,
- 267 • The basal heat flow remains constant through time,
- 268 • The thermal properties of the subsurface at the location of each borehole are
269 uniform and constant through time.

270 In the case of a flat topography, heat transfer could be assumed vertically and the model
271 becomes unidimensional. A change of land use is defined here as a modification of the

272 natural environment at surface, which can affect the shallow subsurface temperature. The
273 temperature variations at surface due to paleoclimates induce a thermal perturbation
274 slowly penetrating the subsurface. This perturbation is used to evaluate the site basal heat
275 flow and subsurface thermal conductivity among boreholes having a similar surface
276 evolution.

277 **4. Results**

278 The temperature profiles undisturbed by heat injection and measured in the GHEs located
279 at the study site in Saint-Lazare-de-Bellechasse are described below with their
280 interpretation, providing a field example to verify the inverse numerical simulation
281 method. Temperature measurements corrected for the depth with equation 1 to take into
282 account the wired probe volume are similar in PG-08-01 and PG-08-2 (Figure 5), except
283 for the depth interval ranging from about 255 to 290 m asl. The observed departure from
284 the expected temperature profile in PG-08-02 is believed to be caused by groundwater
285 flow, which can vary among the two boreholes due to fractured rock heterogeneities.
286 Other than this feature, both temperature profiles show a reversed geothermal gradient
287 with increasing temperature upward from 210 to 280 m asl due to warming at surface.
288 The upper 20 m of the temperature profiles, from 280 to 300 m asl, are further affected by
289 the seasonal temperature variations. Those two temperature profiles that were collected
290 within a few minutes of field work offer the required observations to infer the site heat
291 flow and extent the TRT assessment beyond PG-08-1.

292 **4.1 Evaluation of the site heat flow**

293 Properties of the subsurface model used for inverse numerical simulations to find the heat
294 flow was a thermal conductivity equal to $3.0 \text{ W m}^{-1} \text{ K}^{-1}$, which was evaluated with a
295 conventional TRT in PG-08-01, and a volumetric heat capacity equal to $2.5 \text{ MJ m}^3 \text{ K}$,
296 which was estimated according to a description of the geological materials sampled while
297 drilling [6]. Optimization of the basal heat flow to reproduce the temperature profile in
298 PG-08-01 with the numerical solution considered the observed temperature from 160 to
299 280 m asl. It was not attempted to match the temperature measured in the upper 20 m of
300 the boreholes since this interval is affected by seasonal temperature variations, which are
301 not taken into account by the model upper boundary representing the historic ground
302 surface temperatures. Changes in temperature specified for this boundary are the yearly
303 average temperatures of Figure 2 changed every 5 y or more and extended until year
304 2015, when the temperature profile was measured in PG-08-01. The seasonal temperature
305 variations could have been considered according to the meteorological record but would
306 have increased the simulation time. Matching the upper temperatures affected by the
307 seasonal temperature variations was instead avoided. The absolute temperature value at
308 the upper boundary for the starting point of the simulation was calculated from the initial
309 geothermal gradient condition inferred with the basal heat flow changed every simulation
310 for optimization.

311 The minimum and maximum bound for the basal heat flow optimization was 20 and
312 50 mW m^2 and the optimization started at the lower bound. This range of heat flow was
313 determined from the available heat flow map [23], although data coverage for the studied
314 site is poor. A total of 25 iterations were necessary for the optimization solver to
315 converge toward the solution that provided the best fit with the observed temperatures

316 (Figure 6). The sum of the squared residuals decreased from ~ 13 to 9.3×10^{-2} for the best
317 fit scenario that revealed a basal heat flow converging toward 25 mW m^2 . The initial
318 temperature condition for the best fit scenario was a surface temperature and gradient
319 equal to $6.3 \text{ }^\circ\text{C}$ and $8.3 \times 10^{-4} \text{ }^\circ\text{C m}^{-1}$, respectively (Figure 7).

320 **4.2 Extension of the subsurface thermal conductivity assessment**

321 Inverse numerical simulations to find the thermal conductivity at the location of
322 PG-08-02 were conducted similarly, except that the basal heat flow and the initial surface
323 temperature inferred previously were now treated as input parameters. The model
324 subsurface thermal conductivity was the unknown to find with the optimization process.
325 Observed temperature below the groundwater perturbation (Figure 5) was matched to
326 simulated temperature since conductive heat transfer only was simulated. The minimum
327 and maximum bound for the optimization process was a subsurface thermal conductivity
328 equal to 2.8 and $4.2 \text{ W m}^{-1} \text{ K}^{-1}$ and the optimization started at the lower bound. This
329 range of possible thermal conductivity was determined from geological information about
330 the site bedrock [22], assuming a thermal conductivity range can be assigned to the
331 identified rock type. A total of 24 iterations were needed for the coordinate search solver
332 to converge toward a subsurface thermal conductivity near $3.2 \text{ W m}^{-1} \text{ K}^{-1}$ (Figure 8),
333 decreasing the sum of squared residuals from 2.5×10^{-1} to 2.5×10^{-2} . The initial
334 temperature condition for the best fit scenario was a temperature gradient equal to
335 $7.8 \times 10^{-4} \text{ }^\circ\text{C m}^{-1}$ (Figure 9).

336 The subsurface thermal conductivity estimate obtained at the location of PG-08-02 is
337 within 9 % of that previously measured with a TRT ($3.5 \text{ W m}^{-1} \text{ K}^{-1}$; [6]). The inability to

338 reproduce the observed temperature in the 35 m long section perturbed by groundwater
339 flow may explain the differences in thermal conductivity estimates from the two methods.
340 In order words, the conventional TRT provides an evaluation of the equivalent subsurface
341 thermal conductivity that takes into account groundwater flow, while the estimate
342 obtained with inverse numerical modeling of the temperature profile in PG-08-02
343 neglected advective heat transfer due to groundwater flow. However, both methods
344 yielded thermal conductivity estimates that are sufficiently close to validate the inverse
345 modeling approach, showing its capacity for extrapolation of TRT assessments within
346 boreholes of a given site using temperature profiling undisturbed by heat injection.

347 **5. Discussion and conclusions**

348 A method to make use of temperature profiles in equilibrium with the subsurface and
349 measured in ground heat exchangers (GHEs) was presented in this manuscript to extend a
350 thermal response test (TRT) assessment to other GHEs of the same site. The temperature
351 profiles are measured with a wired probe and corrected for the probe and cable volumes
352 inserted in the GHE piping. The field measurements can be completed within a few
353 minutes, offering accessible data to diversify the methods used for TRT assessments.

354 The observed temperature profiles undisturbed by heat injection of a TRT are reproduced
355 with inverse numerical modeling of conductive heat transfer to infer the site basal heat
356 flow and the subsurface thermal conductivity. The historic ground surface temperature
357 changes and the site topography define the model upper boundary. A first in situ thermal
358 conductivity assessment from a TRT is needed to find the site heat flow with the
359 temperature profile of one GHE. The obtained basal heat flow is subsequently used as an

360 input to find the subsurface thermal conductivity at the location of other GHEs by
361 reproducing the temperature profiles. The optimization of the unknown basal heat flow,
362 in the first case, and the thermal conductivity, in the second case, is achieved with a
363 derivative free solver.

364 The developed methodology was verified at a site located in Saint-Lazare-de-Bellechasse,
365 Canada, where two GHEs had previously been the subject of conventional TRTs. The
366 temperature profiles and the thermal conductivity assessment in the first GHE provided
367 the observations to find the basal heat flow and the thermal conductivity at the location of
368 the second GHE. The subsurface thermal conductivity found by optimization was
369 sufficiently close to that evaluated with the TRT to validate the inverse modeling method.
370 Although uncertainties about the historic ground temperature imposed at the model upper
371 boundary can persist [25], the assessment of the subsurface thermal conductivity can be
372 accurate enough to verify if there are important changes in subsurface properties among
373 different boreholes, as similarly done with pioneer work on thermostratigraphy [17].

374 While this procedure is not expected to replace conventional TRTs, it can find most
375 applications to extent a TRT assessment in large borefields were the performance of
376 several GHEs can be influenced by the heterogeneous subsurface conditions. In cases
377 where there is sufficient information to reduce uncertainty about the site heat flow, the
378 optimization of this parameter may be skipped and the method can potentially replace the
379 conventional TRT to evaluate the subsurface thermal conductivity as done by Rohner et
380 al. [15] on a 300 m deep GHE, but taking into account paleoclimates and surface
381 topography as proposed in this manuscript for shallower boreholes of 139 m depth.
382 However, information about the Earth heat flow can be difficult to find in regions where

383 equilibrium temperature measurements of deep boreholes are sparse, like North East
384 America [28]. In this context, the proposed inverse numerical modeling methodology can
385 be used to extent TRT assessment of any large GHE fields, where more than one
386 evaluation of the subsurface thermal conductivity can be needed. One TRT could be
387 performed in a first GHE and temperature profiles could be measured in all the other
388 GHEs as the borefield is installed to verify if there are significant changes in subsurface
389 thermal conductivity among the borehole locations. The design of the GHE field could be
390 adapted as the analysis of temperature profiles in boreholes reveals the subsurface
391 thermal conductivity distribution. The method could also be used to map the subsurface
392 thermal conductivity in an urban district where the installation of serval ground source
393 heat pump systems is planned. A few TRTs would have to be performed to define the
394 basal heat flow at the district scale and the temperature profiles measured in GHEs could
395 be used to extrapolate the thermal conductivity assessment at the location of each system.
396 The maximum distance between two GHEs for the method to be applicable has not been
397 determined. Giving an exact distance is difficult since it is expected to be affected by the
398 evolution of surface land use that is not directly represented in the model and can affect
399 the subsurface temperature. As long as two GHEs are in an area with a similar basal heat
400 flow and surface land use history, although land use may evolve, the inverse numerical
401 modeling method may offer a descend estimate of the subsurface thermal conductivity.
402 The work presented is a first step to make broader use of temperature profiles in GHEs.
403 The inverse numerical simulation method could be improved to consider groundwater
404 flow, and infer the subsurface hydraulic conductivity when temperature disturbances due
405 to groundwater flow are observed as previously suggested [20]. The simulations could

406 further take into account varying thermal conductivity layers to identify potential
407 subsurface heterogeneities like done for TRT combined with temperature profiling [21].
408 Additional work has to be done to address those issues that can be positively anticipated
409 with the contributions offered by this study. The assessment of the subsurface thermal
410 conductivity in the scope of geothermal heat pump system design can benefit from
411 alternative methodologies that will be further improved.

412 **Acknowledgement**

413 The Banting Postdoctoral Fellowship program, the Natural Sciences and Engineering
414 Research Council of Canada and the *Fonds de recherche du Québec - Nature et*
415 *technologies* are acknowledged for funding this research.

416 **References**

- 417 [1] Mogensen P. Fluid to duct wall heat transfer in duct system heat storages.
418 International Conference on Subsurface Heat Storage in Theory and Practice,
419 Appendix, Part II, Stockholm; 1983, p. 652–7.
- 420 [2] Austin III WA. Development of an in situ system for measuring ground thermal
421 properties. Master Thesis, Oklahoma State University; 1998.
- 422 [3] Gehlin S. Thermal response test - in-situ measurements of thermal properties in hard
423 rock. Licentiate Thesis, Luleå University of Technology, Division of Water
424 Resources Engineering, Department of Environmental Engineering; 1998.
- 425 [4] Spitler JD, Gehlin SEA. Thermal response testing for ground source heat pump
426 systems—An historical review. *Renewable and Sustainable Energy Reviews*
427 2015;50:1125–37. doi:10.1016/j.rser.2015.05.061.

- 428 [5] Rainieri S, Bozzoli F, Pagliarini G. Modeling approaches applied to the thermal
429 response test: A critical review of the literature. HVAC&R Research 2011;17:977–
430 90. doi:10.1080/10789669.2011.610282.
- 431 [6] Raymond J, Therrien R, Gosselin L, Lefebvre R. A review of thermal response test
432 analysis using pumping test concepts. Ground Water 2011;49:932–45.
433 doi:10.1111/j.1745-6584.2010.00791x.
- 434 [7] Kavanaugh SP. Investigation of methods for determining soil formation thermal
435 characteristics from short term field tests. American Society of Heating
436 Refrigerating and Air Conditioning Engineers, Atlanta, RP-1118; 2001.
- 437 [8] Raymond J, Lamarche L. Quality control assessment of vertical ground heat
438 exchangers. ASHRAE Transactions 2014;120:SE – 14–014.
- 439 [9] Moghaddam SMH, Bårman JH. First step towards development of distributed
440 thermal response test using heating cables. Bachelor Thesis, KTH School of
441 Architecture and the Built Environment, Sustainable development, Environmental
442 science and Engineering, Industrial Ecology; 2015.
- 443 [10] Raymond J, Therrien R, Gosselin L. Borehole temperature evolution during thermal
444 response tests. Geothermics 2011;40:69–78.
445 doi:10.1016/j.geothermics.2010.12.002.
- 446 [11] Raymond J, Robert G, Therrien R, Gosselin L. A novel thermal response test using
447 heating cables. Proceedings of the World Geothermal Congress, Bali: 2010, p. 1–8.
- 448 [12] Raymond J, Lamarche L, Malo M. Field demonstration of a first thermal response
449 test with a low power source. Applied Energy 2015;147:30–9.
450 doi:10.1016/j.apenergy.2015.01.117.

- 451 [13] Raymond J, Lamarche L. Development and numerical validation of a novel thermal
452 response test with a low power source. *Geothermics* 2014;51:434–44.
453 doi:10.1016/j.geothermics.2014.02.004.
- 454 [14] Alonso-Sánchez T, Rey-Ronco MA, Carnero-Rodríguez FJ, Castro-García MP.
455 Determining ground thermal properties using logs and thermal drill cutting analysis.
456 First relationship with thermal response test in principality of Asturias, Spain.
457 *Applied Thermal Engineering* 2012;37:226–34.
458 doi:10.1016/j.applthermaleng.2011.11.020.
- 459 [15] Rohner E, Rybach L, Schärli U. A new, small, wireless instrument to determine
460 ground thermal conductivity in-situ for borehole heat exchanger design. *Proceedings*
461 *of the World Geothermal Congress, Antalya: 2005, p. 1–4.*
- 462 [16] Rohner E, Rybach L, Schärli U. Method and device for measuring the temperature
463 or another quantity in a U-shaped geothermal probe and flushing device therefor.
464 *European Patent Office 1600749B1; 2006.*
- 465 [17] Beck AE. The use of thermal resistivity logs in stratigraphic correlation. *Geophysics*
466 1976;41:300–9.
- 467 [18] Kohl T. Transient thermal effects below complex topographies. *Tectonophysics*
468 1999;306:311–24. doi:10.1016/S0040-1951(99)00063-3.
- 469 [19] Kohl T. Palaeoclimatic temperature signals — can they be washed out?
470 *Tectonophysics* 1998;291:225–34. doi:10.1016/S0040-1951(98)00042-0.
- 471 [20] Liebel HT, Huber K, Bjørn SF, Ramstad RK, Bjørge B. Temperature footprint of a
472 thermal response test can help to reveal thermogeological information. *Norges*
473 *Geologiske Undersøkelse Bulletin* 2011;451:20–31.

- 474 [21] Poppei J, Schwarz R, Peron H, Silvani C, Steinmann G, Laloui L, et al. Innovative
475 improvements of thermal response tests. Swiss Federal Office of Energy, Final
476 report; 2008.
- 477 [22] Lebel D, Hubert C. Géologie de la région de St-Malachie (Chaudière-Appalaches).
478 Quebec City, Canada. Gouvernement du Québec, Ministère des Ressources
479 naturelles, Secteur des mines; 1995.
- 480 [23] Majorowicz JA, Grasby SE. Heat flow, depth-temperature variations and stored
481 thermal energy for enhanced geothermal systems in Canada. *Journal of Geophysics
482 and Engineering* 2010;7:232–41. doi:10.1088/1742-2132/7/3/002.
- 483 [24] Beltrami H, Gosselin C, Mareschal JC. Ground surface temperatures in Canada:
484 Spatial and temporal variability. *Geophysical Research Letters* 2003;30:6.1–6.4.
485 doi:10.1029/2003GL017144.
- 486 [25] Chouinard C, Mareschal J-C. Selection of borehole temperature depth profiles for
487 regional climate reconstructions. *Clim Past* 2007;3:297–313. doi:10.5194/cp-3-297-
488 2007.
- 489 [26] COMSOL AB. COMSOL Multiphysics Reference Manual. Stockholm; 2014.
- 490 [27] Conn AR, Scheinberg K, Vicente LN. Introduction to Derivative-Free Optimization.
491 MPS-SIAM Series on Optimization, SIAM, Philadelphia; 2009.
- 492 [28] Blackwell DD, Richards M. Geothermal Map of North America. American
493 Association of Petroleum Geologist:
494 <http://smu.edu/geothermal/2004NAMap/2004NAMap.htm>; 2004.

495

496 **Figure Captions**

497 **Figure 1.** Localisation of the studied site hosting two GHEs numbered PG-08-01 and
498 PG-08-02.

499 **Figure 2.** Ground surface temperature variations inferred by Chouinard and
500 Mareschal[25] from 28 boreholes in the vicinity of the study area.

501 **Figure 3.** Flow chart of the described methodology to extent subsurface thermal
502 conductivity assessments with inverse modeling of temperature profiles.

503 **Figure 4.** Simulation domain, boundary conditions and mesh showing the location of the
504 borehole to reproduce its temperature profile.

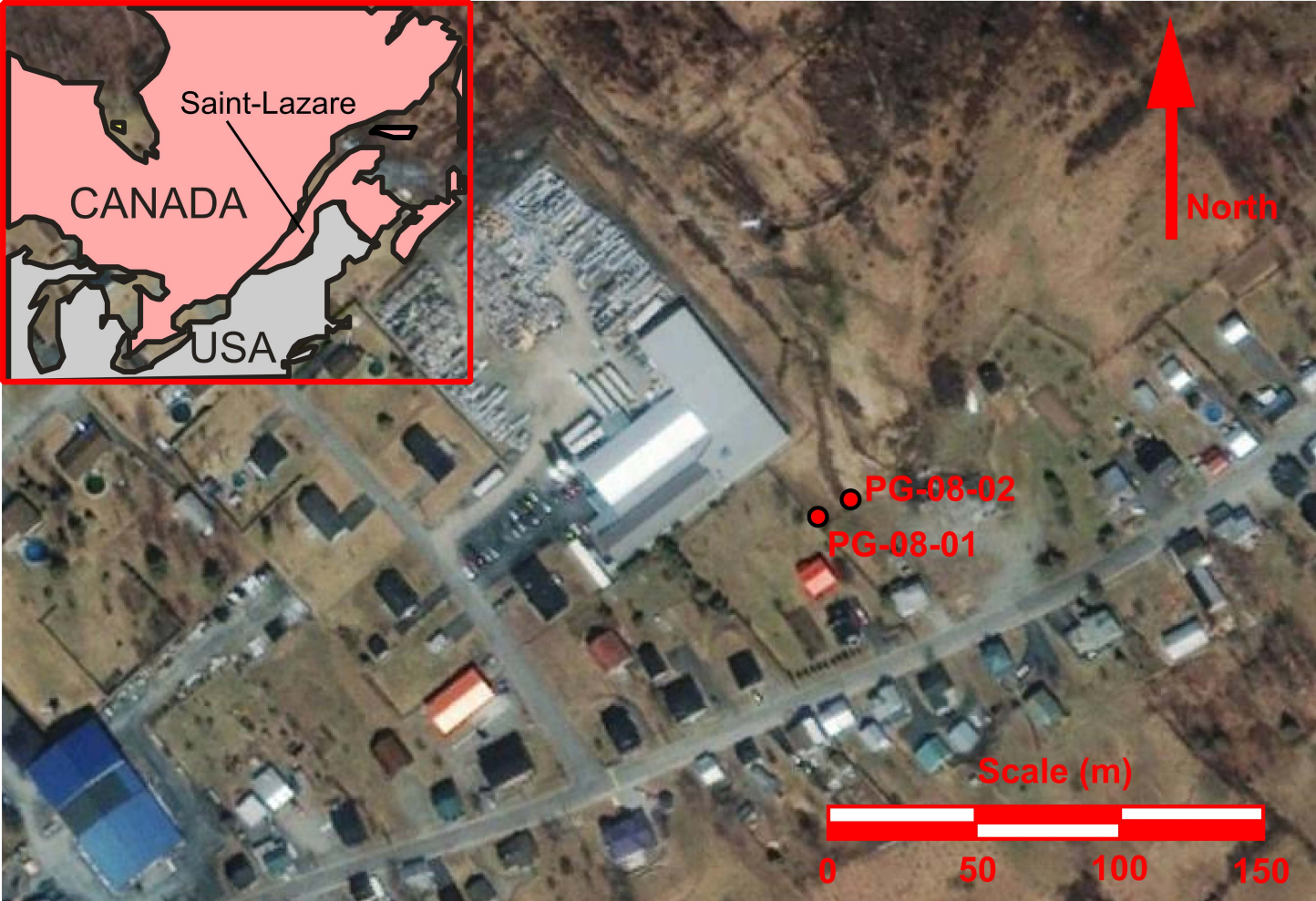
505 **Figure 5.** Temperature profiles in equilibrium with the subsurface corrected for the wired
506 probe volume and recorded in PG-08-01 and PG-08-02.

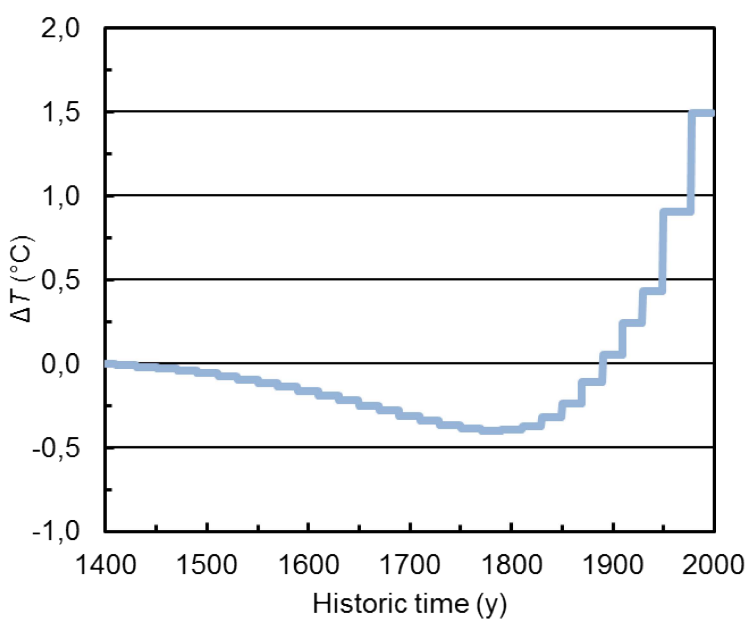
507 **Figure 6.** Histogram of basal heat flow values tried by the coordinate search solver to
508 find the solution that best reproduces temperature measurements in PG-08-01.

509 **Figure 7.** Simulated temperature for the initial condition in 1400 and after the historic
510 ground surface temperature changes in 2015, which are matched to the observed
511 temperature in PG-08-01.

512 **Figure 8.** Histogram of subsurface thermal conductivity values tried by the coordinate
513 search solver to find the solution that best reproduces temperature measurements in
514 PG-08-02.

515 **Figure 9.** Simulated temperature for the initial condition in 1400 and after the historic
516 ground surface temperature changes in 2015, which are matched to the observed
517 temperature in PG-08-02.





- Measurement of temperature profiles in 2 or more GHEs

- Assessment of the subsurface thermal conductivity with a TRT in GHE 1

- Simulation of temperature profile in GHE 1 with inverse modeling of heat transfer

- Identification of the site heat flow

Convergence of the solution

- Simulation of temperature profile in GHE 2 or more with inverse modeling of heat transfer

- Identification of the subsurface thermal conductivity at GHE 2 or more

Convergence of the solution

- Multiple assessment of the subsurface thermal conductivity without repeating TRT

